Article

Modelling Dissolved Oxygen Depression in an Urban River in China

Jingshui Huang [1] [ID], **Hailong Yin** [1,*], **Steven C. Chapra** [2] [ID] **and Qi Zhou** [1]

[1]   College of Environmental Science and Engineering, Tongji University, Shanghai 200092, China; huangjingshui@126.com (J.H.); zhouqi@tongji.edu.cn (Q.Z.)

[2]   Department of Civil and Environmental Engineering, Tufts University, Medford, MA 02155, USA; Steven.Chapra@tufts.edu

*   Correspondence: yinhailong@tongji.edu.cn; Tel.: +86-138-1815-1764

Abstract: Dissolved oxygen (DO) depression in urban rivers appears to be increasing in developing countries, which causes severe aquatic ecosystem stresses. One urban river which suffers DO depression under low flow conditions and requires systematic research for effective mitigation strategies is the Nanfei River (Hefei, China). We investigated its longitudinal profiles of DO and other related water constituents with high spatial resolution monitoring at low flow. A mechanistic DO model for the reach was customized and calibrated with the data obtained. We found that the daily average DO levels within the 11 km study reach shifted from supersaturation (11.5 mg L^{-1}) upstream of the Wangtang Wastewater Treatment Plant (WWTP) to serious depletion (3.6 mg L^{-1}) downstream. Process analysis indicated that DO production via strong algal photosynthesis overwhelmed the DO consumptions upstream from the WWTP. In contrast, DO sources could not compensate for DO consumptions, wherein carbonaceous deoxygenation was the largest consumer of the DO (approximately 70%) downstream the WWTP. Rather than directly contributing labile organics, the WWTP effluent affected the DO balance by shifting the metabolism from upstream autotrophy to downstream heterotrophy. Finally, mitigation strategies for DO depression in rivers in rapidly-urbanizing regions were suggested accordingly.

Keywords: dissolved oxygen; eutrophication; black and odorous water body; WASP model; water quality management

1. Introduction

Dissolved oxygen (DO) depression of surface waters has become one of the most severe environmental problems worldwide. The occurrence of the phenomena will influence biogeochemical cycles of elements and may have severe negative impacts on aquatic ecosystems, such as mortality of benthic fauna, fish kills, habitat loss, and physiological stress [1,2].

The issue was particularly pronounced from the mid-1800s to the 1970s due to the impacts of industrialization and urbanization on rivers, primarily in the West (note that by the West we primarily mean the United States and Europe). Meanwhile, many studies on mechanisms and processes affecting dissolved oxygen deficits in rivers were conducted leading to the development of dissolved oxygen models ([3–10], etc.). The groundbreaking work was the model developed by Streeter and Phelps in 1925 on the Ohio River, which provided a means to evaluate river dissolved oxygen levels [11]. With the breakthrough of computer technology in 1960s, more comprehensive water quality models coupled with the field of operation research were applied to generate cost-effective treatment alternatives (e.g., [12–14]). The focus of the models was on point sources of untreated and primary effluent from the 1920s to the 1970s and secondary effluent from 1970s into the 1980s, and the cleanup implementations

of the urban point sources derived thereof have relieved, or even eliminated, the stress of low dissolved oxygen in many rivers in the West [15,16].

Today, many urban rivers in both undeveloped and developing regions suffer from similar, or even worse, dissolved oxygen depression compared with those in the last century in the West [17,18]. A striking example occurs in China where some highly-polluted rivers are so called 'black and odorous water bodies', with the sensory characteristics of low transparency, high (even "black") chromaticity, and bubbling of stinking gas. In 2015, the State Council of China issued the Action Plan for Prevention and Control of Water Pollution, which set the key indices that, by 2020, the quantity of black and odorous water bodies in built-up areas in cities at prefecture level and above will be controlled within 10% and, by 2030, generally eliminated [19]. The motivation for remediating black water bodies has been strongly supported by all political levels, from the central to the local government. Now the question comes: can we copy the experience of the mitigation strategy from Europe or North America? Here, the situation differs from the former oxygen deficit problems of the West in many aspects.

First, the population in urban areas in the developing countries now are much denser than that in the past in the West, which will intensify the conflict between water resource development and water environmental conservation. Second, there are some special remaining issues in the booming cities within only two or three decades in the developing countries, such as short-sighted urban planning, lack of municipal infrastructure, unreasonable or outdated locations of factories, landfills, and wastewater treatment plants, poor villages situated inside the city waiting for renewal, so called 'urban villages' and so on. Third, the corresponding legislation and investment lag behind the present speed of increasing productivity and the lack of environmental protection awareness result in historical accumulations of air, water and soil pollution, e.g., contaminated sediments. Fourth, the environmental debts during the rapid industrialization and urbanization period cause the subsequent environmental problems to be more complicated and interdependent. The effects of the cleanup of urban point sources on the mitigation of hypoxia remains uncertain. Finally, yet importantly, due to the urgency of cleanup and the booming economic growth, the decisions and funds for mitigation are now, or will soon be, readily available in the transitional regions. Additionally, since we live in an era of information explosion, more knowledge and techniques of pollution control are accessible now. Therefore, even though oxygen models have been applied to many rivers in the West, it is still essential to set up oxygen models to investigate the mechanisms of oxygen depression in a typical urban river and provide corresponding policy suggestions in the transitional regions.

The greater Yangtze River Delta metropolitan region is the most important economic center of China. It has the highest urbanization and population density. It is particularly suitable for initiating such an investigation, because black and odorous water bodies are common and funds for mitigation are more readily available than in other developing countries.

As a sub-center city of the region, Hefei City has evolved into the most rapidly urbanized and populated prefecture-level cities. In the past ten years, the city's size has been expanding dramatically, where the population increased by 70% to 7.8 million and gross domestic product (GDP) increased by 560% to 82 billion US dollars in 2015 compared with those in 2005 [20]. However, the long-term ignorance of environmental issues has led to severe environmental degradation. The Nanfei River, the mother river of Hefei City, not only faces increasing water scarcity due to extensive water consumption by the growing population and industry, but is also heavily polluted because it receives large amounts of wastewater from the city. The consequences are the shifts of the water quality from the drinking water reservoir to the black and odorous water body within 11 km of the urban section of the river.

The goal of our research is to obtain a longitudinal profile of dissolved oxygen to quantify the shift of the water quality under low flow condition in the urban section of the river. Based on that, we seek to establish an overarching budget of dissolved oxygen to identify the main sources and sinks with an oxygen model. Finally, it is intended to provide a basis for general mitigation strategies and policy recommendations for oxygen depression of urban rivers in transitional regions.

2. Materials and Methods

2.1. Study Site

The Dongpu Reservoir upstream of the Nanfei River is a drinking water reservoir with storage of 242 million m^3, which intercepts most of the clean upland water, except during floods (Figure 1). An urban village about 3 km downstream from the Dongpu Reservoir (between sites 2 and 3, Figure 1), directly discharges sewage after primary treatment (mentioned as 'untreated wastewater' in the context) through a drain into the river. A sealed landfill site is located about 5 km downstream from the Dongpu Reservoir (between sites 5 and 6). The Wangtang Wastewater Treatment Plant (mentioned as 'WWTP' in the context below as it is the only WWTP in the research domain) is situated about 6 km downstream from the reservoir (at site 6). It discharges treated wastewater from a population of more than 300,000 people (treatment capacity of 200,000 m^3 d^{-1}), which results in a wastewater effluent that accounts for about 60% of the total annual discharge and constitutes about 75% of the discharge to the river during the low flow periods [21]. The Wangtang WWTP utilizes an oxidation ditch treatment process with a nitrification/denitrification unit resulting in removal efficiencies of 95% for biological oxygen demand (BOD) and 80% for total [22]. Approximately 7.5 km downstream from the reservoir, the Nanfei River receives its first tributary, the Sili River (between sites 10 and 11). There is another drinking water reservoir called the Dafangying Reservoir upstream of the Sili River, which impounds its upland water as well (Figure 1).
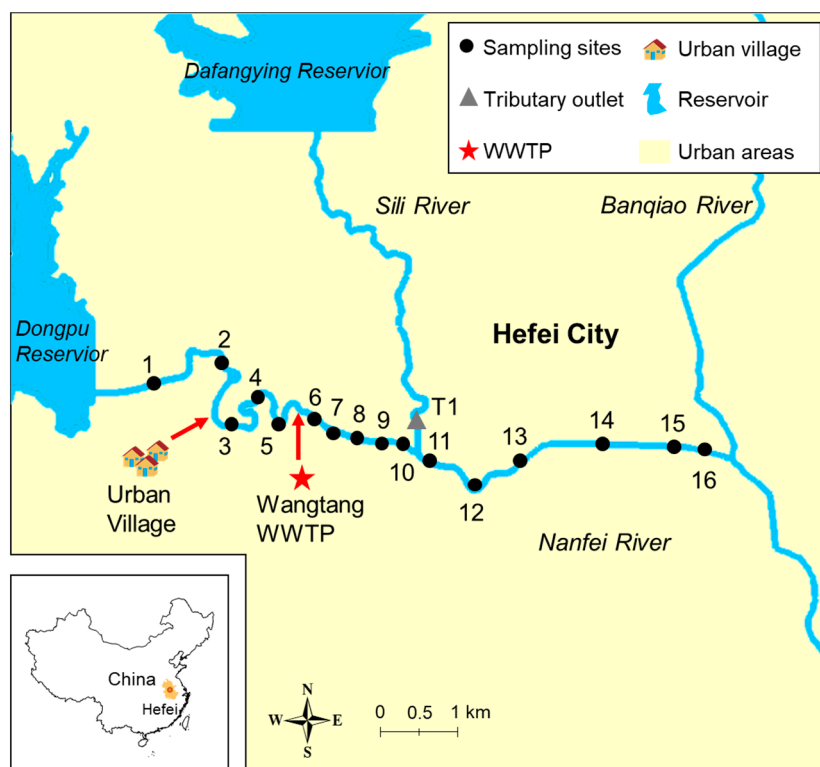

Figure 1. Nanfei River system, land use, sampling sites in Hefei City, China.

In the reach from 7.5 km to 11 km downstream from the reservoir (between sites 11 and 16), the waterway is channelized and receives no point sources since sewage interception engineering was implemented during the national 11th Five-Year Plan before 2011. However, several pumping stations are distributed in this reach, which discharge storm water together with combined sewer overflow (CSO) to prevent the city center from flooding during rain events. The final river section (between sites 15 and 16) shifts to 'black and odorous' with bubbles visible to the naked eyes on the water

surface. Next, another tributary, the Banqiao River, joins the Nanfei River about 11 km downstream from the reservoir. A rubber dam is installed 17 km downstream from the reservoir (out of the map extent in Figure 1) and its height is controlled daily by the operators from the Hefei Urban Drainage Management Authority according to the regulations of the 'Rubber Dam Operation Procedures for the Nanfei River'. Its main function is to maintain the depth of the river in the urban section in order to protect the urban landscape.

2.2. Field Program and Lab Analysis

Considering the artificial control of the water depth and the stable inflow from the wastewater treatment plant, the hydrodynamics of the river is relatively stable the whole year except during the peak flow period. The river's hydrograph for 2015 is presented in the Supplementary Files (Figure S1). The components and the composition of the pollutants from the Wangtang WWTP effluents remain almost constant over time because of the stable operation of the treatment processes. Therefore, the Nanfei River is an ideal model system to offer insight into spatial variations of the processes, which are involved in the DO balance within an urban river under the low flow conditions.

On the basis of this initial assessment, an intensive hydrological and water quality survey was conducted in the dry season from 3 to 6 October 2015 to obtain the longitudinal profile of DO and other process-related variables in the Nanfei River under low flow conditions. The results were further employed to customize and constrain the mechanistic model.

2.2.1. Hydrology

The river hydrological conditions, including flow, velocity and depth, were investigated using a surveying vessel equipped with a RiverSurveyor system (Sontek ADP, San Diego, CA, USA) at sites 1, 5, 10, 15, as well as the Sili River outlet during the same sampling period. Gauge readings for water level at site 14 were acquired from the Hefei Bureau of Hydrology and Water Resources Survey. Data for daily discharge and the concentration of constituents for the Wangtang WWTP effluent were obtained from the Hefei Urban Drainage Management Authority. The flow of the untreated wastewater was estimated by the population living in the urban area and per capita sewage discharge estimates.

2.2.2. Sampling Sites and Water Analyses

Diurnal variations were recorded by taking bihourly samples along the 10 km river section at 16 selected study sites as well as the Sili River outlet and the urban sewers (Figure 1). There was a two-hour window during sampling as two groups of three people drove up and down the reach from one site to another. One group took samples from sites 1 to 10, while another from sites 11 to 16. The start time of the sampling was 11 a.m. and the end time was 9 a.m. the next day. The total number of samples were 228. Samples were obtained by collecting river water with a bucket from bridges or the riverbanks. The bridge samples were taken in the middle of the cross-section width. All samples were taken at 0.5 m under the water surface. All samples were preserved in a 4 °C fridge before being transported to the laboratory.

Temperature, pH, DO, and electrical conductivity (EC) were measured in the field using a HACH HQ40D portable meter (Loveland, CO, USA). Nitrogen and phosphorus speciation, that is total phosphorus (TP), dissolved inorganic phosphorus (DIP), total nitrogen (TN), NO_2^-, NO_3^-, and NH_4^+ (sum of NH_3 and NH_4^+) were analyzed by the methods of Chinese National Standards [23]. Five-day carbonaceous biological oxygen demand ($CBOD_5$) was determined after five-days of sample incubation using a polarographic DO meter for DO measurement at site 1, untreated wastewater outfalls and the Sili River outlet. Chlorophyll-a (Chl-a) concentration was measured by pulse amplitude modulation (WALTZ PAM-2000, Effeltrich, Germany). Dissolved organic carbon (DOC) was measured using a total organic carbon analyzer (SHIMADZU TOC-L, Kyoto, Japan). Chloride (Cl^{-1}) was measured using ion chromatography (DIONEX ICS-3000, Waltham, MA, USA). All of the analyses were performed in duplicate.

2.3. Measurement of Key Model Parameters

In order to lower the uncertainty of calibrated model parameters, the critical parameters related to the DO processes, including spatial nitrification rates, carbonaceous deoxygenation rates, and sediment oxygen demands (SOD) were measured with laboratory incubations in the 2015 low flow surveys.

Water samples from sites 3 and 6 were incubated to measure the nitrification and carbonaceous deoxygenation rates. The water sample preparation and laboratory protocol used to quantify carbonaceous deoxygenation and nitrification rates was closely followed by Chen et al. [24] with minor modifications to suit local conditions in this study. Sediments were dredged at sites 1, 2, 3, 4, 7, 14, 15, and 16 and sealed in ice and wrapped with aluminum foil, and transported to the lab. Two liters of bulk river water were simultaneously collected at the same sites. The SODs at different sites were determined following the lab protocol and calculation method reported by Sharma et al. [25]. A detailed description of the incubation methods and results is presented in the Supplementary Files (Figures S2 and S3).

3. Model Customization and Calibration

Considering the steady-state condition during the dry periods in the Nanfei River described above and the objective of insight into spatial variations of the DO processes in this study, the model was run time-variably with constant inputs to reach a steady-state condition.

3.1. Hydraulic Model

Since the hydrodynamics are such that the gradients are most important in the longitudinal direction, a one-dimensional, cross-sectional averaged, time independent hydrodynamic model was set up using the 'EPDRiv1' software (Atlanta, GA, USA). The hydrodynamic model solves the 1D shallow water equations with a finite difference scheme in a control volume [26]. The domain started from the reservoir outlet and down to the rubber dam (about 17 km) with 72 nodes with an average intermodal distance of approximately 220 m. The detailed descriptions of the cross-sections (i.e., station and elevation pairs) were obtained from the former bathymetric survey with a spatial resolution of 50–100 m from the Urban Drainage Management Authority of Hefei. The flow boundary conditions of the upstream and the Sili River were obtained by the hydrological survey measured data. The water level boundary condition of the downstream was taken from the gauge reading at the rubber dam. The boundary conditions of the WWTP effluent and untreated wastewater discharge were described above in the section 'Hydrology'. The Manning friction coefficient in the hydrodynamic model was calibrated with the simulated results against the measured flow, velocity and depth data at sites 5, 10, and 15. After calibration, the simulated velocity and depth of each segment were provided for the setup of mass transport and water quality model.

3.2. Mass Transport Model

Cl^- is a conservative constituent with dilution and external loading as the only processes affecting its concentration. The mass transport model calibration used chloride data to adjust the longitudinal dispersion coefficient under low flow conditions. The results developed from the analyses were then used in the subsequent water quality simulations.

3.3. Water Quality Model

The water quality model was set up with WASP 7.5.2 (Atlanta, GA, USA), which simulates multiple water quality constituents with its EUTRO module [27]. The EUTRO program contained physical-chemical processes which can affect the transport and interaction among the nutrients, phytoplankton, carbonaceous material, and dissolved oxygen in the aquatic environment. It can simulate the nutrient enrichment, eutrophication, and DO depletion processes. Additionally, the

spatial heterogeneity of CBOD deoxygenation rate and SOD can be presented by setting different rate values in different segments. Therefore, it is suitable for this study.

The water quality model has 45 segments (corresponded to the hydrodynamic model segmentation), with the upstream boundary at the reservoir outlet and downstream boundary at the confluence of the Banqiao River (approximately 11 km).

The upstream and downstream boundary conditions were obtained from water quality data at sites 1 and 16, respectively. The loadings from the untreated wastewater from the urban village, the WWTP effluent, and the Sili River were calculated by multiplying the measured concentrations by their corresponding flows. For each segment, SOD flux was interpolated from the measured SOD values at different measurement sites. The loadings of $CBOD_u$, NH_4^+, and SOD fluxes in the different segments are shown in Figure 2. The nitrification rate value of 0.16 d^{-1} derived from the measurement at site 6 was used in the model calibration (see Supplementary Files). The CBOD deoxygenation rates of 0.3 d^{-1} and 0.09 d^{-1} derived from the incubation at sites 3 and 6 were used for labile and refractory CBOD loadings, respectively (see Supplementary Files). $CBOD_u$ concentrations of the boundary conditions were converted from the measured $CBOD_5$ values with first order decay equation and the measured CBOD decay rates.
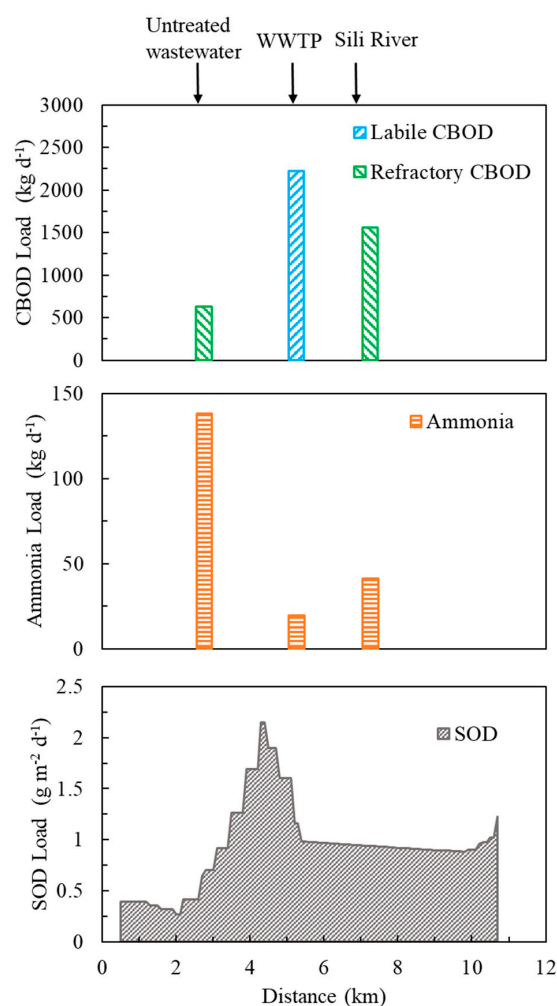

Figure 2. Pollutant loadings of the Nanfei River.

The temperature inputs were obtained by linearly interpolating the measured temperature at different sites. The average solar radiation measured for the study area during the survey period was 530 Langley d^{-1} [28]. The average photoperiod for the survey was 0.5.

3.4. DO Processes Analysis

The theory behind the DO modelling using WASP 7.5.2 is well documented in its users' manual [27]. The DO is calculated by taking into account processes of algal respiration and photosynthesis, CBOD deoxygenation, nitrification, sediment oxygen demand, and air-water flux. The processes involved in the DO balance are presented in Figure 3.
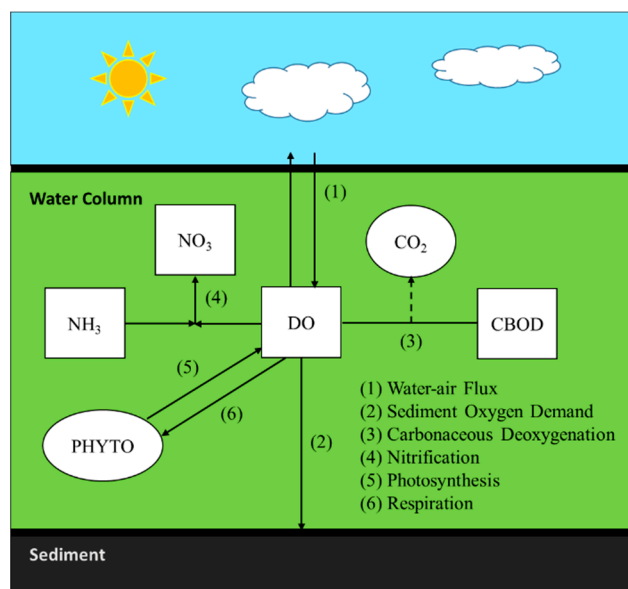

Figure 3. Schematic description of the processes involved in the DO balance (modified from the WASP user's manual [27]).

Once the model was calibrated, the contributions of the different processes to the DO profile were then quantified. All the biogeochemical transformation fluxes were divided by the surface area of the river bed and were provided in g O m^{-2} d^{-1}.

The metabolism of each segment was determined by the ratio of areal rate of system primary production to respiration (P:R). If the ratio is more than 1 in the segment, its metabolism is autotrophic. Otherwise its metabolism is heterotrophic. The system primary production is expressed as algal photosynthesis, whereas the system respiration is expressed as the sum of the algal respiration, CBOD deoxygenation and sediment oxygen demand, with the fluxes of all the processes given in g O m^{-2} d^{-1}.

3.5. Model Application

The base scenario was defined using the values of this survey under low flow conditions. Different scenarios of mitigation measures were evaluated compared with the baseline scenario.

The effect of sludge dredging was assessed under the baseline scenario by setting the SOD fluxes in each segment to a reference value in the most upstream segment, namely 0.27 g m^{-2} d^{-1}. The policy proposal of upgrading the water quality of WWTP effluent from the 1A grade of WWTP effluent discharge standard to the fourth grade of the surface water quality standard, which means that the concentrations of CBOD$_u$ and total phosphorus in the WWTP effluent are reduced from the current level to 6 mg L^{-1} and 0.3 mg P L^{-1}, respectively [29]. Thereby the effect of the WWTP upgrade on the DO level is evaluated by running the model with the boundary conditions mentioned above. The scenario of the untreated wastewater interception was set up under the baseline by removing the flow and loading of the untreated wastewater from the urban village. The measures of the polluted tributary clean-up will be simulated by setting the CBOD$_u$ concentration of the Sili River to 10 mg L^{-1} according to the 1A grade of the WWTP effluent discharge standard [30] and meanwhile setting the CBOD deoxygenation coefficient to 0.073 d^{-1} [31]. The measure of increasing in-stream flow will be

simulated by setting the upstream boundary condition of flow to 5.57 m^3 s^{-1}, which fits a real previous water diversion condition. Under this scenario, the hydrodynamic model was run first to give the updated hydraulic information needed for the water quality model simulation.

4. Results and Discussion

4.1. Calibration Model Results

In order to calibrate the model, model outputs were compared with measurements. Mean concentrations and standard deviations at the longitudinal sampling sites, correlation between simulated and measured concentrations, bias, and root-mean-square error (RMSE) were calculated at all the sites to assess the performance of the models (Table 1).

Table 1. Statistics calculated on observed and simulated variables: mean values ($\overline{C_{obs}}$, $\overline{C_{sim}}$) and standard deviations (σ_{obs}, σ_{sim}) of observed and simulated concentrations, correlation, bias, and RMSE.

Variable	Unit	$\overline{C_{obs}}$	$\overline{C_{sim}}$	σ_{obs}	σ_{sim}	ρ	Bias	RMSE
Flow	m^3 s^{-1} (except for ρ)	1.93	2.02	1.61	1.65	1.00	0.09	0.13
Depth	m (except for ρ)	1.93	2.13	1.25	1.37	0.99	0.20	0.25
Velocity	m s^{-1} (except for ρ)	0.08	0.03	0.03	0.01	0.61	−0.05	0.05
Chloride	mg L^{-1} (except for ρ)	40.3	40.68	15.30	16.13	0.99	0.38	1.81
DOC	mg L^{-1} (except for ρ)	4.93	5.54	1.51	2.21	0.97	0.61	1.00
NH$_4^+$	mg N L^{-1} (except for ρ)	1.46	1.66	2.43	2.20	0.99	0.20	0.43
NO$_{23}$	mg N L^{-1} (except for ρ)	7.15	7.10	3.95	3.85	1.00	−0.05	0.26
DIP	mg P L^{-1} (except for ρ)	0.46	0.45	0.15	0.19	0.89	−0.01	0.09
TP	mg P L^{-1} (except for ρ)	0.57	0.60	0.13	0.13	0.91	0.03	0.06
Chl-a	μg L^{-1} (except for ρ)	41.2	44.31	54.78	55.60	0.99	3.11	7.35
DO	mg L^{-1} (except for ρ)	7.43	7.47	2.73	2.55	0.99	0.04	0.44

4.1.1. Hydrodynamics

As shown in Figure 4, the model is able to reproduce the hydrodynamics well. The Manning friction coefficient was set to 0.05 for the whole reach.
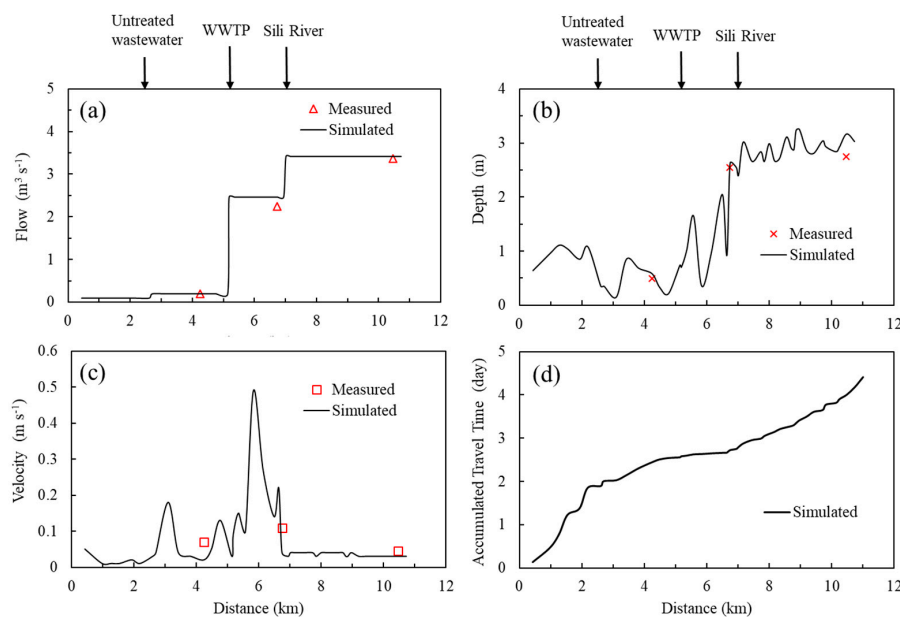

Figure 4. Measured and simulated hydrodynamic conditions in the Nanfei River. (**a**) Flow; (**b**) depth; (**c**) velocity and (**d**) accumulated travel time (only simulated).

Under low flow conditions, the inflow from the upstream reservoir was very small (Figure 4a). The river received untreated wastewater from the urban village with the discharge of 0.1 m³ s⁻¹. Notably, the WWTP effluent was the largest contributor of the river flow (2.24 m³ s⁻¹, 66%). The polluted tributary joined the main stem with the discharge of 0.95 m³ s⁻¹.

Figure 4b shows the simulated and observed water depth at three sites. The mean depth of the river in the upper 7 km reach ranged from 0.1 to 2 m, while it remained approximately 3 m with small changes in the lower reach. The upper 7 km reach meanders with a natural bank; however, since the lower reach flows through the city center, it is artificially channelized and stratified with the concrete riverbank for flood prevention. Additionally, it was once deepened for shipping.

A peak in velocity occurred at about 6 km (Figure 4c). The reason was that an abrupt change of the river bottom elevation forms a waterfall with the height of about 1 m near there. Downstream of that, the velocity stabilized between 0.03 and 0.04 m/s. The small velocity of the whole reach could be attributed to the upstream reservoir impounding and the river elevation controlled by the downstream rubber dam.

The simulated travel time is shown in Figure 4d. The long travel time upstream of the WWTP effluent brought up the hint that longitudinal dispersion should not be ignored with respect to mass transfer in this reach.

4.1.2. Mass Transport

Subsequent model calibration analyses using chloride data as a conservative tracer were conducted to adjust the longitudinal dispersion coefficient. Figure 5a shows the model results matching the chloride data under the low flow conditions. The final longitudinal coefficient (5 m² s⁻¹) was used in the segments upstream of the WWTP outlet.

The concentration of chloride in the most upstream was approximately 10 mg L⁻¹. This increased gradually due to the influence of the untreated wastewater discharge and longitudinal dispersion. Then it was elevated steeply by the WWTP effluent to 51 mg L⁻¹ and remained at this level downstream.

Based on the observed and predicted flow, depth, velocity, and chloride values, the model predictions are good and we, therefore, assume that the model is able to provide basic estimates for the mass transport of the simulated water quality constituents.

4.1.3. Water Quality Constituents

As the DO balance involves several highly non-linear physical and biogeochemical processes (Figure 3), the DO levels are affected by many other water quality constituents and respond to their variations, either directly or indirectly. Therefore, even though the DO is the most important parameter in this study, the model performances of the other relative water quality parameters were examined as well to make sure that the model reliably reproduces the DO processes. In this sense, DO concentrations are the end results of the model.

Figure 5b–h show the model results compared with field data for seven water quality parameters in the water column: DOC, ammonia, nitrite/nitrate, orthophosphate, total phosphorus, chlorophyll a, and dissolved oxygen. The model is shown to reproduce the longitudinal pattern of the simulated variables properly. The simulated increases and drops of the variable concentrations are synchronized with the observed trends. A list of crucial stoichiometric and kinetic coefficients related to DO balance in the study river is provided in Table 2.
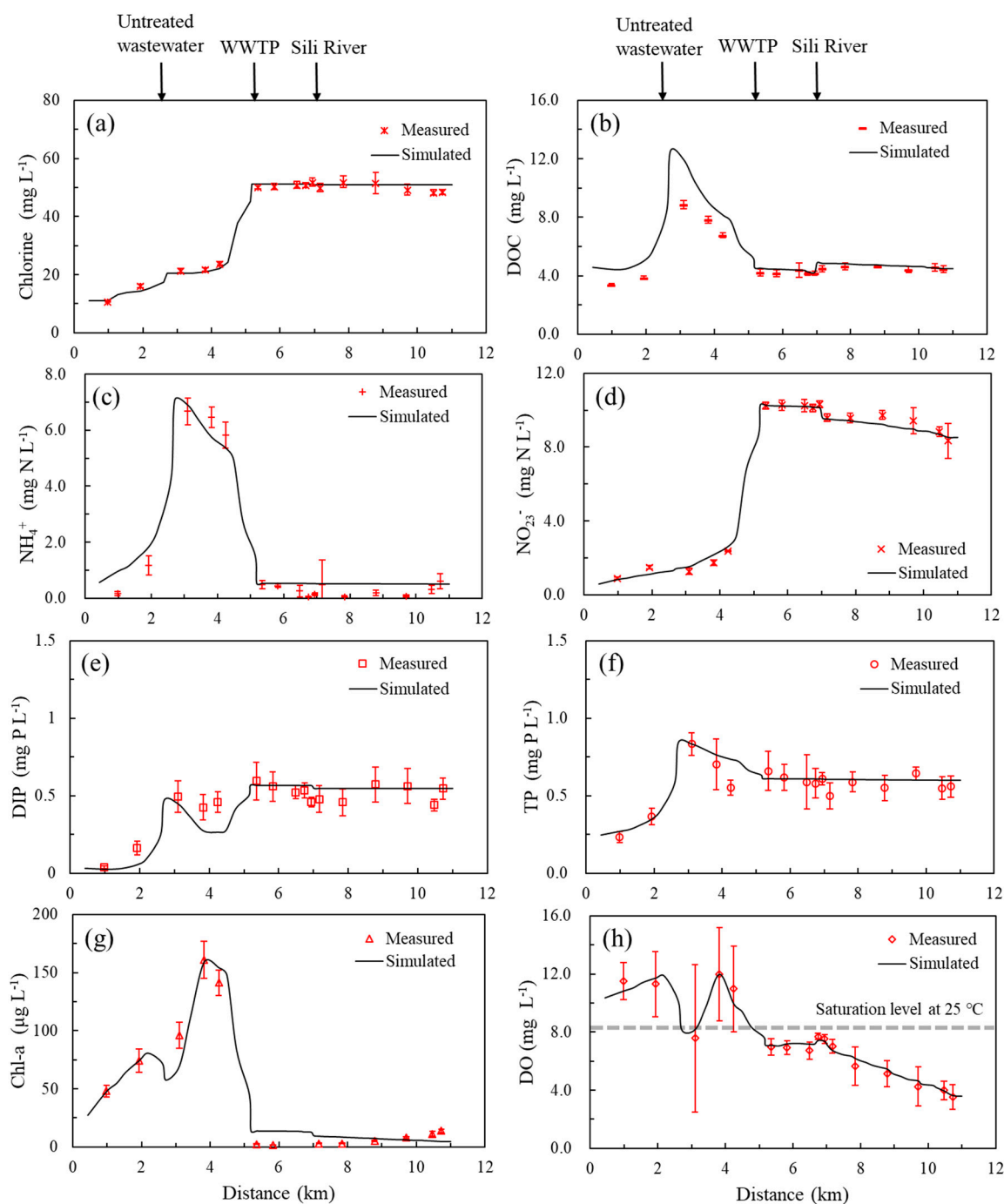
Figure 5. Measured and simulated concentrations of the related water quality constituents. (**a**) Cl⁻; (**b**) DOC; (**c**) NH_4^+; (**d**) sum of NO_2^- and NO_3^-; (**e**) DIP; (**f**) TP; (**g**) Chl-a and (**h**) DO. Error bars represent standard deviations of bi-hourly observed data. Grey dash line in panel (**h**) represents DO saturation level at 25 °C.

Table 2. Stoichiometric and kinetic parameters related to DO balance in the model.

Parameters	Unit	Optimal Value
Nitrification rate constant at 20 °C	d^{-1}	0.16
Nitrification temperature coefficient	-	1.045
Half saturation constant for nitrification oxygen limit	$mg\ O\ L^{-1}$	1.5
Phytoplankton maximum growth rate constant at 20 °C	d^{-1}	2.9
Phytoplankton growth temperature coefficient	-	1.07
Phytoplankton endogenous respiration rate constant at 20 °C	d^{-1}	0.125
Phytoplankton respiration temperature coefficient	-	1.045
Phytoplankton maximum death rate constant	d^{-1}	0.4
Phytoplankton carbon to Chlorophyll ratio	-	50
Phytoplankton half-saturation constant for nitrogen uptake	$mg\ N\ L^{-1}$	0.015
Phytoplankton half-saturation constant for phosphorus uptake	$mg\ P\ L^{-1}$	0.035
Algal shade multiplier [1]	-	0.0587
Algal shade exponent	-	0.778
Algal self-shading method [1]	-	See ref. [15]
Phytoplankton optimal light saturation	Langley	250
Calculation of reaeration method	-	O'Connor-Dobbins [2]
Reaeration temperature correction	-	1.03
Waterfall reaeration water-quality coefficient [3]	-	1
Waterfall reaeration dam-type definition	-	0.8
Waterfall elevation	m	1
Calculation of hydraulic reaeration [3]		See ref. [15]
Refractory CBOD decay rate constant at 20 °C	d^{-1}	0.09
Refractory CBOD decay rate temperature correction coefficient	-	1.045
Refractory CBOD half saturation oxygen limit	$mg\ O\ L^{-1}$	0.5
Labile CBOD decay rate constant at 20 °C	d^{-1}	0.3
Labile CBOD decay rate temperature correction coefficient	-	1.045
Labile CBOD half saturation oxygen limit	$mg\ O\ L^{-1}$	0.5

[1–3] The algal self-shading calculation method, the O'Connor-Dobbins equation, and the calculation of hydraulic re-aeration can be referred to Chapra [15].

The DO level in the most upstream 2 km (between sites 1 and 2) was supersaturated due to low concentrations of oxygen-consuming substances and strong phytoplankton photosynthesis. The untreated wastewater discharge with high concentrations of organic pollutants and nutrients has a significant impact on the downstream water quality. The concentrations of DOC, ammonia, and orthophosphate in the river increased sharply. The decrease of DO level from sites 2 to 3 was caused by the oxidation of the fast labile CBOD and the nitrification of the ammonia discharged from the untreated wastewater. At site 3, the DO concentration fell back to a saturated condition, yet had a large diurnal fluctuation due to the oxygen production-consumption cycle by the autotrophic and heterotrophic aquatic organisms. Meanwhile, the excessive nutrients (especially phosphorus) heightened phytoplankton growth. The phytoplankton bloomed at site 4. Again, the DO concentration peaked and reached supersaturated level due to strong primary production. From sites 4 to 5, as the algal biomass declined, the photosynthetic source of DO decreased. In addition, carbonaceous deoxygenation, ammonia nitrification, and the contaminated sediment near the sealed landfill site further consumed oxygen. As a result, the DO level dropped sharply, and near the WWTP effluent outlet, the DO level increased close to saturation. Due to the large discharge of the WWTP effluent and its negligible concentration of algae, the Chl-a concentration was diluted strongly and remained low downstream. As a result, the contribution from phytoplankton photosynthesis to DO concentration downstream was less influential. Due to the low concentration of ammonia and the slow decay rate of the refractory CBOD in the effluent, there was no significant change of the DO concentration from site 6 to site 8. The small but abrupt elevation of DO level to saturation concentration at about 6.5 km was caused by the waterfall, which increased the re-aeration rate. However, since the river received the pollutants from the polluted tributary at site 11 (about 7 km), the daily average DO level was gradually

depleted to approximately 3.6 mg L^{-1} at site 16 in the most downstream section, where the water turned darker. The DO depression in the water column not only influenced the visual appearance of the river but also brought a severe threat to the living aquatic organisms in that stretch. For instance, dead fish were observed floating on the water surface.

4.2. Processes Affecting River DO Balance

The concentration of oxygen in the river is a product of air-water fluxes, physical transport, and biogeochemical processes, including CBOD deoxygenation, nitrification, SOD, algal respiration, and photosynthesis. Due to the accuracy of the simulation results of the related constituents, we conclude that the model is able to identify the important processes responsible for development of DO deficit and provide good estimates of the river metabolism.

Figure 6 shows the relative dominance of the sources and sinks of DO in the Nanfei River. Since the untreated wastewater discharges a high concentration of labile CBOD, the areal rate of DO consumption by CBOD deoxygenation downstream of the urban village outfall is 2–3 times (7.21 g m^{-2} d^{-1}) higher than upstream. Even though the WWTP effluent contributes the largest loading of CBOD to the Nanfei River (Figure 3), the areal rate of CBOD deoxygenation downstream from the WWTP outfall is much lower than upstream. The reason is that WWTPs can remove labile CBOD in the raw sewage through conventional treatment processes and discharge relatively refractory CBOD in the effluent [31]. However, the Sili River brings in a large amount of labile CBOD from its non-regulated drainage area, which makes CBOD deoxygenation the largest consumer of DO (approximately 70%) in the downstream reach.
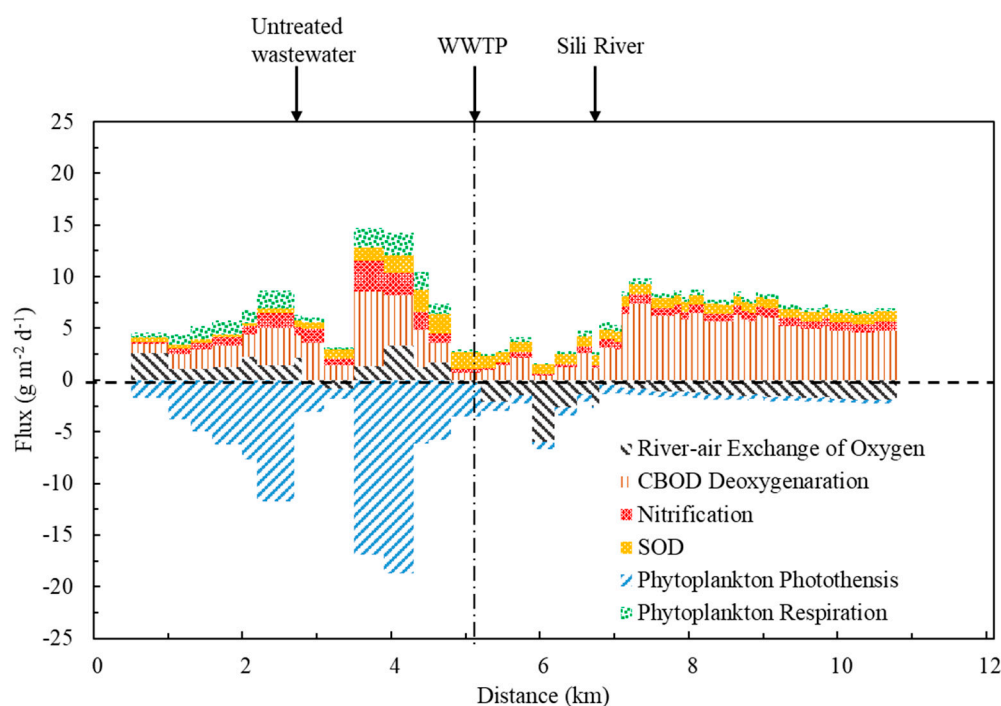

Figure 6. Areal rates of various DO sources and sinks under low flow conditions.

The largest areal rate of oxygen consumption by nitrification is the section downstream the urban village outfall due to the high concentration discharge of ammonia from the untreated wastewater and favorable environmental conditions. Since the treatment processes in the WWTP have the capability of nitrogen removal, the discharge concentration of ammonia is very low (0.1 mg L^{-1}) and actually dilutes ammonia to a lower level downstream. Therefore, nitrification contributes a small proportion (less than 20%) of oxygen depletion downstream of the WWTP outfall.

Sediments serve as the ultimate repository of many of the pollutants discharged to aquatic systems [32]. In the 2.5 km most upstream section, the SOD accounts for less than 10% of the DO consumption due to the less contaminated sediments in the area. Downstream of the urban village outfall, the areal rate of SOD increases by three times than that upstream. The largest areal rate of SOD occurs approximately 500 m upstream of the WWTP outfall. This is due to a legacy repository of organic matter in the sediments adjacent to the sealed landfill, which reveals the issue of historical pollution accumulation during the rapid urban development period. SOD is the second largest oxygen consumer downstream of the WWTP effluent until the end of the study reach. Sharma et al. reported that the SOD rates were higher below wastewater discharges and tributary confluences [25]. In addition to the above explanations, the high SOD areal rates between the two tributaries (7–11 km) can be attributed to the combined sewer overflow discharge from the distributed pumping stations along the riverbank. Due to the water level control by the rubber dam, the particulate organic matters discharged during CSO events settle, nourish the biological reactor, and subsequently promote oxygen depletion through remineralization in the sediments [33,34].

Algal respiration and photosynthesis rates are proportional to phytoplankton biomass. Therefore, the peaks of DO consumption and production by algal respiration and production are synchronized with the peaks of Chl-a (Figure 5). Upstream of the WWTP, algal primary production dominates the DO balance because it exceeds the sum the of the DO consumption by all the other processes, which results in supersaturated DO in this reach. The strong primary production is the result of long residence time (approximately eight days under low flow conditions), favorable climatic conditions (i.e., high temperatures and maximum daily solar radiation), and the additional nutrient inputs discharged from the untreated wastewater. In contrast, the DO production by photosynthesis drops abruptly downstream of the WWTP effluent due to the section's low algal concentration. Thus, in a similar fashion to upstream, the photosynthesis gains cannot compensate for the larger DO consumption.

The river-air exchange of oxygen from the water column to the atmosphere is due to the supersaturated DO level in the water column caused by the pure oxygen production from algal photosynthesis, whereas the flux of oxygen (i.e., re-aeration) from the atmosphere to the water column is driven by the water-column oxygen deficit. The fluxes are out of the water upstream of the WWTP effluent because of the strong primary productivity in the section. Downstream of the WWTP effluent, a re-aeration peak occurs where the waterfall is situated as the increased velocity and the hydraulic turbulence enhances re-aeration. However, the re-aeration rate in the reach between the two tributaries decreases significantly because of the low river velocity. In the end, the production cannot offset the consumption of DO in the river, which leads to the depletion and depression of DO in the urban section of the Nanfei River.

4.3. Effects of Effluents on DO Balance of the Nanfei River

Effluent discharges can cause large perturbations to river metabolism and to the subsequent DO balance, through the direct impact of large nutrient and organic inputs or by altering extrinsic factors, such as water temperature, hydrologic characteristics, light availability, bacterial levels, and so on [35]. However, the effects of effluents on river metabolism were not consistent in previous studies. Bernot et al. found that both production and respiration rates increase in response to the disturbances [36]. Ruggiero et al. and Izagirre et al. showed that sewage inputs in streams could induce higher heterotrophic activity and ecosystem respiration rates [37,38]. In contrast, a study of the Seine River reported that the river system is heterotrophic upstream from the WWTP effluent and autotrophic in the downstream sector during low-flow periods [39].

In our study, the WWTP effluent has a significant dilution effect on the abundance of primary producers in the downstream receiving water because of its large discharge and its negligible concentration of phytoplankton biomass. Moreover, previous studies indicated that large amounts of heterotrophic biomass are discharged to the system from the effluent [40,41]. Therefore, since the WWTP effluent contributes more than 70% of the total flow of the Nanfei River, it is strongly believed

that heterotrophic bacteria are dominant rather than primary producers downstream from the WWTP in the Nanfei River. At low flow, the system is heterotrophic downstream from the WWTP effluent, with a ratio of oxygen production to consumption lower than 0.5 (Figure 7). Even though the WWTP effluent contains substances such as refractory CBOD and low concentrations of ammonia, which consume small amounts of oxygen, it does affect the DO balance and significantly alters the river metabolism. In conclusion, the WWTP effluent creates a net heterotrophic ecosystem downstream in the Nanfei River.
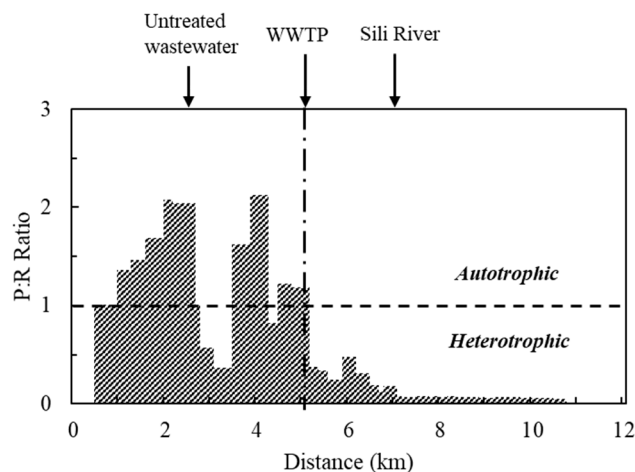
Figure 7. Longitudinal primary production to the respiration ratio and metabolism condition.

However, in terms of the effect of the untreated wastewater discharge on the river metabolism, the story is quite different. The primary productivity is restricted by the low ambient nutrient concentrations in the most upstream 2-km reach, where the P:R ratio is approximately 1. After receiving the untreated wastewater with a large amount of nutrient and organic inputs, both heterotrophic and the autotrophic activity rates are promoted. Even so, primary production outpaces respiration, making the ratio more than 1 (P:R > 1), which causes supersaturation near the discharge. This provides a pertinent example of the conclusion that the system shifts from net heterotrophy to net autotrophy induced by the wastewater.

Based on the two distinctive results from the above examples, the effects of the wastewater on the river metabolism and, subsequently, DO balance, are inconclusive. They are additionally dictated by other factors, such as flows, environmental temperature, light availability, nutrient and organic matter levels upstream and in the effluents.

4.4. Model Application: Engineering Controls

Based on the analyses of DO balance elaborated above, we developed some scenarios of engineering control measures to assess their mitigation effects on DO depression in the Nanfei River. The selected engineering controls in the scenario analysis are as follow: (i) WWTP upgrade; (ii) control of SOD through sludge dredging; (iii) interception of untreated wastewater from the urban village; (iv) clean-up measures of the polluted tributary; and (v) in-stream flow increase.

In more developed regions of China, the local governments are ambitious to upgrade WWTP effluents from 1A of the WWTP effluent discharge standard to fourth grade of the surface water quality standard [29,30]. As a result, the DO level is slightly elevated in this scenario (Figure 8). Actually, the wastewater treatment processes are currently advanced with limited room for improvement. Considering the efforts and effects of WWTP upgrade, it is uneconomic and inefficient.
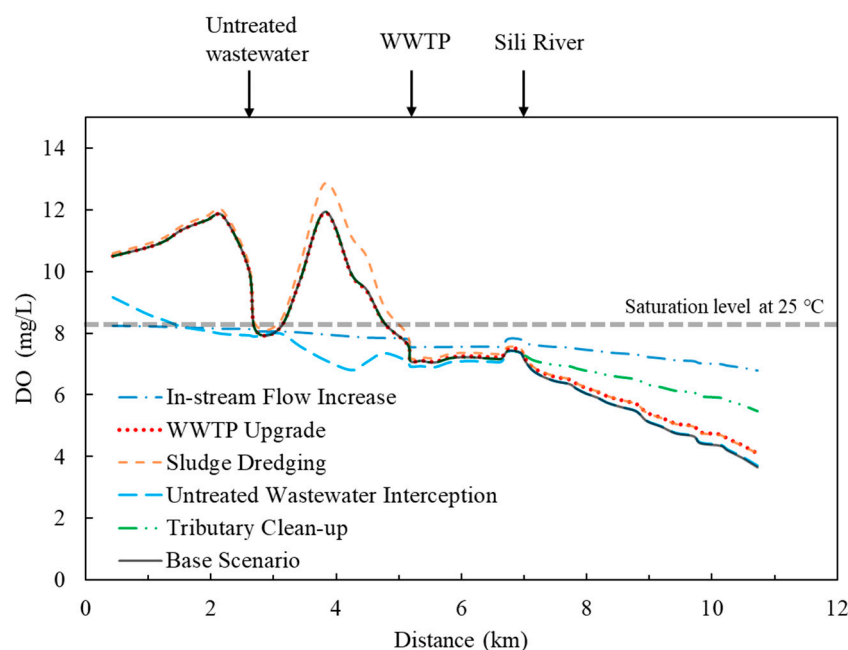
Figure 8. Scenario analysis of engineering controls for DO level improvement in the Nanfei River. Grey dash line represents DO saturation level at 25 °C.

Control of SOD through sludge dredging is a common, though costly, river clean-up measure. The scenario analysis results show that the effects of the DO elevation in the downstream section are insignificant, as well (Figure 8).

The model reveals that the interception of the untreated wastewater from the urban village changes the supersaturated DO condition in the upstream reach significantly (Figure 8). However, it has a negligible effect on the DO level downstream. After interception, the nutrient and organic inputs will be significantly reduced. Thus, phytoplankton growth will be restricted by the limited nutrients and subsequently blooms will be mitigated. On the other hand, less oxygen will be consumed due to the reduction of the labile CBOD and ammonia discharge. Therefore, there will be no hypoxia or supersaturated fluctuations in this section. Eutrophication could cause episodic oxygen depletion in the system, which could be shifted to hypoxia with physical processes that restrict water exchange [42]. In this sense, despite the negligible mitigation of hypoxia in the downstream reach, it is of great importance to restore a healthy aquatic ecosystem in the upstream reach through the interception of the untreated wastewater.

The polluted tributary clean-up may be the preferred option according to the scenario analysis. The overall DO levels downstream are elevated to above 5 mg L^{-1} (Figure 8), which meets the third grade of the Chinese surface water standard [29]. During China's 11th Five-Year Plan (2005–2010), the Hefei City government started to invest in implementing interception of the sewers along the riverbank. It is reasonable that the projects usually focus on the main stem of the urban river. Thereby, the tributaries still suffer from raw sewage discharge and bring in large amounts of labile organic matter to the main stem at their confluence.

Due to the interception of the upstream drinking water reservoir, the Nanfei River severely lacks in-stream flow and becomes effluent-dominated. The scenario analysis of in-stream flow increase showed that the DO depletion was significantly alleviated in the downstream. The DO levels were above the 5 mg L^{-1} threshold of the third grade of the Chinese surface water standard [29]. The clean flow from upstream strengthened the re-aeration by an increase of the velocity, lowered the hydraulic and pollutant residence time, and increased the dilution capacity of pollutants in the whole reach. Therefore, it had obvious effects of DO level improvement. It is understandable to fulfil the human need in a booming and densely populated city at the first place. On top of that, if the reservoir

could release more water from upstream considering the environmental and ecological need, the environmental stresses in the study reach, such as DO depression would be relieved to some extent.

To conclude, in order to mitigate the DO depression of the Nanfei River urban section, the most straightforward and effective first step is to clean up the polluted tributary. In terms of the upstream aquatic system health, untreated wastewater should be intercepted considering the current eutrophication situation and internal feedback mechanisms, such as legacy storage of excess detritus from phytoplankton and microbes in the sediments [1].

4.5. Policy Suggestions

Dissolved oxygen deficit is a simple, but effective, indicator of the water quality, which reflects various watershed pollution issues comprehensively [43]. As the Nanfei River is a typical urban river in China, its DO depression indicates some challenges widely faced by urban rivers in rapidly transitioning regions:

- Lack of a clean upstream inflow affects the DO level by greatly reducing the dilution capacity of receiving pollutants, lowering the velocity, and then decreasing the re-aeration rate and increasing the residence time of the pollutants in the river. The reason behind that is the shortage of water resources caused by booming urban populations. The priority task of the clean water resources is to fulfil the needs of urban life and productivity, rather than to consider the ecological water demand of the river.
- SOD consumes large amount of DO in the river section adjacent to the sealed landfill in the upstream reaches of the Nanfei River because of the historical pollution accumulation in the sediments. Several decades ago, the site of the sealed landfill was far from the Hefei City urban area, whereas nowadays it has become part of the urban area due to rapid urbanization. However, the historical pollution accumulation in the river will not vanish due to unanticipated urban expansion and short-sighted urban planning. On the contrary, it waits for solutions.
- Even though the WWTPs were built in the Hefei City with advanced and stable treatment processes, serious DO deficits still occur. A most critical reason behind this is that the low wastewater collection rate due to the incomplete municipal pipe network offsets the benefits of the WWTPs. According to our scenario analysis results, the untreated wastewater interception from the urban village and the polluted tributary have the most significant effects on the mitigation of DO deficits. This underscores the importance of social resource distribution and of infrastructure construction investments by decision-makers.

Since implementation of secondary treatment for WWTPs in the U.S., the DO depletion has been significantly alleviated and the percentage of reaches characterized by desirable DO (above the 5 mg L^{-1} threshold) increased [44]. However, obviously, the establishment of WWTP with tertiary treatment could not solve the DO deletion issue in our study reach once and for all. Back to the question in the beginning, can we copy the experience of the mitigation strategy from Europe or North America? The answer is no. Establishing WWTP to mitigate DO depletion is a valuable experience that we obtained and put into practice. Nevertheless, corresponding measures and policies based on the actual local situations should be considered simultaneously.

According to the present case study, some suggestions to mitigate the DO depression in the urban rivers in the rapidly transitioning countries are proposed as follows: (i) to promote water resource optimal allocation and water conservation, considering the need of both the booming population and river ecological health; (ii) to make reasonable and balanced investments on infrastructure construction with priority for efficiency in mitigating the DO deficits; and (iii) to envisage and solve the historical pollution accumulation problems during the rapid urbanization, such as the untreated wastewater discharge from the urban village, the contaminated sediments near the sealed landfill and so on.

A key to success would be to build a well-designed monitoring network along the rivers that would enable the reliable customization of the process-based model. The present study provides

valuable mitigation strategies and policy suggestions for DO depression in the urban rivers by providing insight into the underlying causal processes. Similar situations and mitigation strategies to that seen and implemented in China are likely present in other of the world's transitional regions. This would ideally tackle a representative set of other water quality issues such as eutrophication, heavy metals, biocides, pharmaceuticals, and persistent organic pollutants, which are often accompanied by sewage discharge, through the implementation of the mitigation strategies to DO depression in the aquatic systems [45].

Supplementary Materials: The following are available online at www.mdpi.com/2073-4441/9/7/520/s1, Figure S1: Hydrograph at site 16 in the Nanfei River in 2015, Figure S2: Measured SOD flux rates at sites 1, 2, 3, 4, 7, 14, 15 and 16, Figure S3: Derivation of CBOD deoxygenation rates and nitrification rates at sites 3 and 6.

Author Contributions: Jingshui Huang suggested the idea; Jingshui Huang, Hailong Yin and Qi Zhou organized the field survey; Jingshui Huang performed the lab analysis; Hailong Yin, Steven S. Chapra. contributed to the model set up and calibration; Jingshui Huang analyzed the data; Jingshui Huang. wrote the paper; and HailongYin and Steven S. Chapra. revised and improved the manuscript.

Conflicts of Interest: The authors declare no conflict of interest.

References

1. Diaz, R.J. Overview of hypoxia around the world. *J. Environ. Qual.* **2001**, *30*, 275–281. [CrossRef] [PubMed]

2. Zhang, J.; Gilbert, D.; Gooday, A.J.; Levin, L.; Naqvi, S.W.A.; Middelburg, J.J.; Scranton, M.; Ekau, W.; Pena, A.; Dewitte, B.; et al. Natural and human-induced hypoxia and consequences for coastal areas: Synthesis and future development. *Biogeosciences* **2010**, *7*, 1443–1467. [CrossRef]

3. Theriault, E.J. The oxygen demand of polluted waters, I. Bibliographical, A critical review, II. Experimental, The rate of deoxidation. In *Public Health Bulletin No. 173*; U.S. Public Health Society: Washington, DC, USA, 1927; p. 85.

4. Velz, C.J. Deoxygenation and reoxygenation. *Trans. Am. Soc. Civ. Eng.* **1939**, *104*, 560–572.

5. Velz, C.J. Factors influencing self purification and their relation to pollution abatement. *Sew. Works J.* **1947**, *19*, 629–644.

6. O'Connor, D.J.; Dobbins, W.E. Mechanism of reaeration in natural streams. *Trans. Am. Soc. Civ. Eng.* **1958**, *123*, 641–666.

7. Owens, M.; Edwards, R.; Gibbs, J. Some reaeration studies in streams. *Int. J. Air Water Poll* **1964**, *8*, 469–486.

8. Department of Scientific and Industrial Research. *Effects of Polluting Discharges on the Thames Estuary*; H.M. Stationery Office: London, UK, 1964; p. 609.

9. O'Connor, D.J. The temporal and spatial distribution of dissolved oxygen in streams. *Water Resour. Res.* **1967**, *3*, 65–79. [CrossRef]

10. Bowie, G.L.; Mills, W.B.; Porcella, D.B.; Campbell, C.L.; Pagenkopf, J.R.; Rupp, G.L.; Johnson, K.M.; Chan, P.W.H.; Gherini, S.A.; Chamberlin, C.E. *Rates, Constants, and Kinetic Formulations in Surface Water Quality Modeling*; EPA/600/3-85/040; U.S. Environmental, Protection Agency: Athens, GA, USA, 1985.

11. Streeter, H.W.; Phelps, E.B. *A Study of the Pollution and Natural Purification of the Ohio River. III Factors Concerned in the Phenomena of Oxidation and Reaeration*; U.S. Department of Health, Education & Welfare: Washington, DC, USA, 1925; Volume 146, pp. 1–75.

12. Thomann, R.V.; Sobel, M.J. Estuarine water quality management and forecasting. *J. Sanit. Eng. Div.* **1964**, *90*, 9–38.

13. Deininger, R.A. Water Quality Management—The Planning of Economically Optimal Pollution Control Systems. Ph.D. Thesis, Northwestern University, Evanston, IL, USA, 1965.

14. ReVelle, C.S.; Loucks, D.P.; Lynn, W.R. A management model for water quality control. *J. Water Pollut. Control Fed.* **1967**, *39*, 1164–1183. [PubMed]

15. Chapra, S.C. *Surface Water-Quality Modeling*; Waveland Press: Long Grove, IL, USA, 2008.

16. Stoddard, A.; Harcum, J.B.; Pagenkopf, J.R.; Simpson, J.; Bastian, R.K. *Municipal Wastewater Treatment: Evaluating Improvements in National Water Quality*; John Wiley & Sons: New York, NY, USA, 2002.

17. Yang, C.; Lung, W.; Kuo, J.; Liu, J. *Water quality modeling of a hypoxic stream. Practice Periodical of Hazardous, Toxic, and Radioactive Waste Management*; American Society of Civil Engineers: Reston, VA, USA, 2005; Volume 14, pp. 115–123.

18. Cox, B.A. A review of dissolved oxygen modelling techniques for lowland rivers. *Sci. Total Environ.* **2003**, *314–316*, 303–334. [CrossRef]

19. The State Counsil of China. *Action Plan for Prevention and Control of Water Pollution*; People's Publishing House: Beijing, China, 2015.

20. Hefei Bueau of Satistics; Hefei Statistics Survey Team of National Bueau. *2015 Hefei Statistical Yearbook*; China Statistics Press: Beijing, China, 2016.

21. Huang, J.; Yin, H.; Jomma, S.; Rode, M.; Zhou, Q. Identification of Pollutant Sources in a Rapidly Developing Urban River Catchment in China. In Proceedings of the EGU General Assembly, Vienna, Austria, 17–21 April 2016.

22. Introduction to Wangtang Wastewater Treatment Plant. Available online: https://wenku.baidu.com/view/5d866bab551810a6f52486cc.html (accessed on 30 May 2017).

23. Environmental Protection Agency of China. *The Monitoring and Analysis Method for Water and Wastewater*, 4th ed.; China Environmental Science Press: Beijing, China, 2002.

24. Chen, C.-H.; Lung, W.-S.; Yang, C.-H.; Lin, C.-F. Spatially variable deoxygenation in the danshui river: Improvement in model calibration. *Water Environ. Res.* **2013**, *85*, 2243–2253. [CrossRef] [PubMed]

25. Sharma, K.; Mceachern, P.; Spafford, M.; Zhu, D.; Yu, T. Spatial Variation of Sediment Oxygen Demand in Athabasca River: Influence of Water Column Pollutants. In Proceedings of the World Environmental and Water Resources Congress, Kansas City, MO, USA, 17–21 May 2009.

26. NRE Icp. *A Dynamic One-Dimensional Model of Hydrodynamics and Water Quality EPD-RIV1 Version 2.1 Technical Manual*; Georgia Envionmental Protection Division: Atlanta, GA, USA, 2014.

27. Wool, T.A.; Ambrose, R.B.; Martin, J.L.; Comer, E.A. *Water Quality Analysis Simulation Program (WASP) Version 6.0 Draft: User's Manual*; US Environmental Protection Agency—Region 4: Atlanta, GA, USA, 2002.

28. Weast, R.C.; Astle, M.J. *CRC Handbook of Chemistry and Physics*; CRC Press, Inc.: Boca Raton, FL, USA, 1980.

29. Environment Protection Agency of China. *The Environment Quality Standards for Surface Water (GB 3838-2002)*; Ministry of Environmental Protection of the People's Republic of China: Beijing, China, 2002.

30. Environment Protection Agency of China. *Discharge Standard of Pollutants for Municipal Wastewater Treatment Plant (GB 18918-2002)*; Ministry of Environmental Protection of the People's Republic of China: Beijing, China, 2002.

31. Lung, W.-S. *Water Quality Modeling for Wasteload Allocations and TMDLs*; John Wiley & Sons, Inc.: New York, NY, USA, 2001.

32. Ditoro, D.M. Sediment flux modeling. *Soil Sci.* **2001**, *168*, 75–76.

33. Turner, R.E.; Rabalais, N.N.; Justic, D. Gulf of mexico hypoxia: Alternate states and a legacy. *Environ. Sci. Technol.* **2008**, *42*, 2323–2327. [CrossRef] [PubMed]

34. Xue, C.; Yin, H.; Xie, M. Development of integrated catchment and water quality model for urban rivers. *J. Hydrodyn. Ser. B* **2015**, *27*, 593–603. [CrossRef]

35. Carey, R.O.; Migliaccio, K.W. Contribution of wastewater treatment plant effluents to nutrient dynamics in aquatic systems: A review. *Environ. Manag.* **2009**, *44*, 205–217. [CrossRef] [PubMed]

36. Bernot, M.J.; Sobota, D.J.; Hall, R.O.; Mulholland, P.J.; Dodds, W.K.; Webster, J.R.; Tank, J.L.; Ashkenas, L.R.; Cooper, L.W.; Dahm, C.N.; et al. Inter-regional comparison of land-use effects on stream metabolism. *Freshw. Biol.* **2010**, *55*, 1874–1890. [CrossRef]

37. Ruggiero, A.; Solimini, A.G.; Carchini, G. Effects of a waste water treatment plant on organic matter dynamics and ecosystem functioning in a mediterranean stream. *Ann. Limnol.-Int. J. Lim.* **2006**, *42*, 97–107. [CrossRef]

38. Izagirre, O.; Agirre, U.; Bermejo, M.; Pozo, J.; Elosegi, A. Environmental controls of whole-stream metabolism identified from continuous monitoring of basque streams. *J. N. Am. Benthol. Soc.* **2008**, *27*, 252–268. [CrossRef]

39. Vilmin, L.; Flipo, N.; Escoffier, N.; Rocher, V.; Groleau, A. Carbon fate in a large temperate human-impacted river system: Focus on benthic dynamics. *Glob. Biogeochem. Cycle* **2016**, *30*, 1086–1104. [CrossRef]

40. Raimonet, M.; Vilmin, L.; Flipo, N.; Rocher, V.; Laverman, A.M. Modelling the fate of nitrite in an urbanized river using experimentally obtained nitrifier growth parameters. *Water Res* **2015**, *73*, 373–387. [CrossRef] [PubMed]

41. Petersen, T.M.; Rifai, H.S.; Suarez, M.P.; Stein, A.R. Bacteria loads from point and nonpoint sources in an urban watershed. *J. Environ. Eng.* **2005**, *131*, 1414–1425. [CrossRef]

42. Diaz, R.J.; Rosenberg, R. Spreading dead zones and consequences for marine ecosystems. *Science* **2008**, *321*, 926–929. [CrossRef] [PubMed]

43. Sánchez, E.; Colmenarejo, M.F.; Vicente, J.; Rubio, A.; García, M.G.; Travieso, L.; Borja, R. Use of the water quality index and dissolved oxygen deficit as simple indicators of watersheds pollution. *Ecol. Indic.* **2007**, *7*, 315–328. [CrossRef]

44. U.S. Environmental Protection Agency. *Progress in Water Quality: An Evaluation of the National Investment in Municipal Wastewater Treatment*; U.S. EPA, Office of Water: Washington, DC, USA, 2000.

45. Pernet-Coudrier, B.; Qi, W.; Liu, H.; Müller, B.; Berg, M. Sources and pathways of nutrients in the semi-arid region of Beijing-Tianjin, China. *Environ. Sci. Technol.* **2012**, *46*, 5294–5301. [CrossRef] [PubMed]